Numerical simulation of evolution of steam-water two-phase zone in a fractured geothermal reservoir by considering capillary pressure effects

Yohei TATEISHI[1], Ryuichi ITOI[1], Toshiaki TANAKA[1], Junichi TAKAYAMA[2]

[1] Department of Earth Resources Engineering, Faculty of Engineering, Kyushu University, Fukuoka 819-0395, Japan

[2] Nittetsu Mining Co., Ltd., Chiyoda-ku, Tokyo 100-8377, Japan

y-tateishi@mine.kyushu-u.ac.jp

Keywords: *numerical model, steam-water two-phase zone, capillary pressure*

ABSTRACT

Pressure drawdown in a geothermal reservoir due to production operations may lead to a formation of steam-water two-phase zone in the shallower parts of the reservoir as has been observed in the Wairakei geothermal field in New Zealand and in the Ogiri geothermal field in Japan. In this study, we carried out numerical simulations using a three dimensional reservoir model for investigating the influences of steam and water capillary pressure on the evolution of two-phase zone in the shallower parts of the reservoir.

A developed three dimensional reservoir model consists of a cap rock and fracture systems, and was made in reference to the field data obtained from the Ginyu fault zone of Ogiri. The Ginyu fault plays the main reservoir for steam production with temperatures around 230^{o}C. Pressure and temperature profiles of the well in the exploration stage suggest that there was a steam-water two-phase zone below a low permeable cap rock in the shallow zone of this reservoir.

Production and reinjection simulations with the developed numerical model to examine the growth of two-phase zone in reservoir by incorporating the effects of steam and water capillary pressure into the model were carried out. The results indicated a vertical extension of the two-phase zone due to pressure drawdown in the fracture part of the model. Also, the vaporization front is shown to progress slowly in the model compared to that without the effects of capillary pressure. Capillary pressure lowers the vapor pressure which then allows the liquid phase water to exist even the surrounding pressure reaches to saturated with respect to its temperature.

1. INTRODUCTION

The Ogiri geothermal field is located in Kagoshima prefecture, southern Kyushu, Japan. The reservoir lies along the Ginyu fault, which is the main geologic feature of the field. Relationships of estimated formation temperature and pressure of wells in the Ogiri field shows that most of the Ogiri geothermal reservoir is of liquid-dominated type; however, there are a few two-phase zones with a vapor-static pressure distribution above the liquid-dominated zones. Through fumaroles and zones of hydrothermal alteration, which are manifestation at the surface of Ginyu fault, it was estimated that there are high permeability conduits in the cap rock connecting the surface and the Ogiri geothermal reservoir (Yano et al., 1995).

We developed a three-dimensional model which can represent these phenomena of the Ogiri geothermal reservoir and used the 2-dimensional model by Yano et al. (1995) as a reference. They conducted simulation to find out what conditions control a formation of the two-phase zones in natural-state. Their study showed that the deep recharge rate and the permeability of the conduit in the cap rock have significant effects on the development of the two-phase zones in the reservoir like Ginyu fault. We improved their model to three-dimensional model and analyzed the behavior of the two-phase zone of each layer in production and reinjection simulation

Capillary pressure is defined to be the pressure difference between steam and liquid phases. It also plays an important role in controlling fluid distributions and recoveries in petroleum and geothermal reservoirs. Urmeneta et al. (1997) studied the role of capillary pressure through one and two-dimensional models of porous media. They found that capillary pressure tends to keep the steam in the fractures and the liquid in the matrix. In their model, they used van Genuchten equation (van Genuchten, 1980) for the matrix blocks and linear function for the fracture blocks for the capillary pressure functions. We used their model to determine the capillary pressure functions in our model. In our study, we incorporated the capillary pressure functions into the three-dimensional model and evaluated the behavior of the two-phase zones in production and reinjection simulations.

2. CHARACTERISTICS OF THE OGIRI FIELD

Kodama and Nakajima (1988) described the development survey at the Ogiri geothermal field. The Ogiri geothermal reservoir is characterized by a fault system that includes the Ginyu fault. Figure 1 shows estimated formation temperatures for well located in Ogiri field based on logging, production, geochemical and geological data. The wells in the Ginyu field show steep temperature gradients between 200m a.s.l. and 500m a.s.l. and constant temperature around 230°C below sea level elevation. The pre-exploitation subsurface temperature distribution in Ogiri features a high temperature zone in the eastern part of the field with temperature decreasing to the west. This implies that the heat source is associated with the volcanoes at the eastern of the Ogiri field and that hot water upflow occur along the Ginyu fault and other sub-vertical faults. In the Ginyu reservoir, there is a high permeability reservoir and a low permeability cap rock in the shallower parts of the reservoir. The cap rock spreads above the eastern Ginyu fault. It prevents meteoric water to flow down into the reservoir keeping the formation of the reservoir to develop.

Figure 2 shows the relationship between elevation and measured feedpoint pressures in wells drilled along Ginyu and Shiramizugoe reservoirs. For the Ginyu reservoir the pressure gradient is larger than the hydrostatic gradients for a 232°C water column. This implies that significant upflow is present in the Ginyu reservoir. Figure 2 also shows that the pressure and elevation relationship is nearly vapor-static in the upper part of the Ginyu reservoir. Pressure and

temperature profiles of the well in the exploration stage suggest that there was a steam-water two-phase zone below low permeable cap rock in the shallow zone of this reservoir. Figure 3 shows a conceptual model of the Ginyu field made by Yano et al. (1995) and expresses the characteristics and the geology of the reservoir.

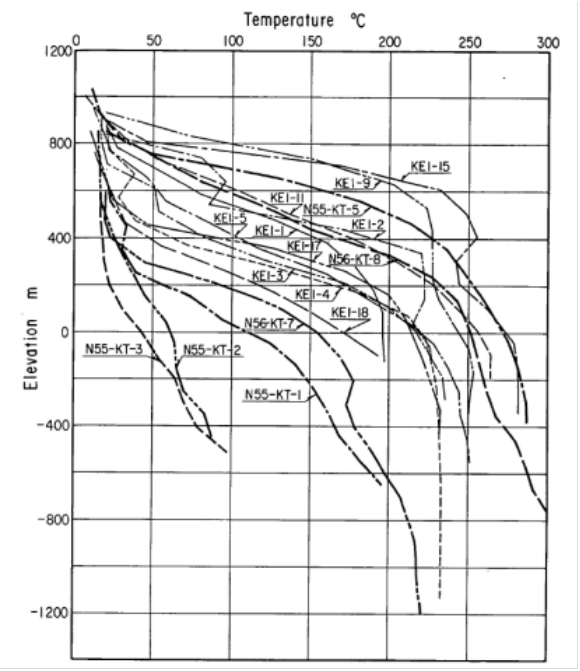

Figure 1: Estimated formation temperature of wells at the Ogiri field (Kodama and Nakajima, 1988).

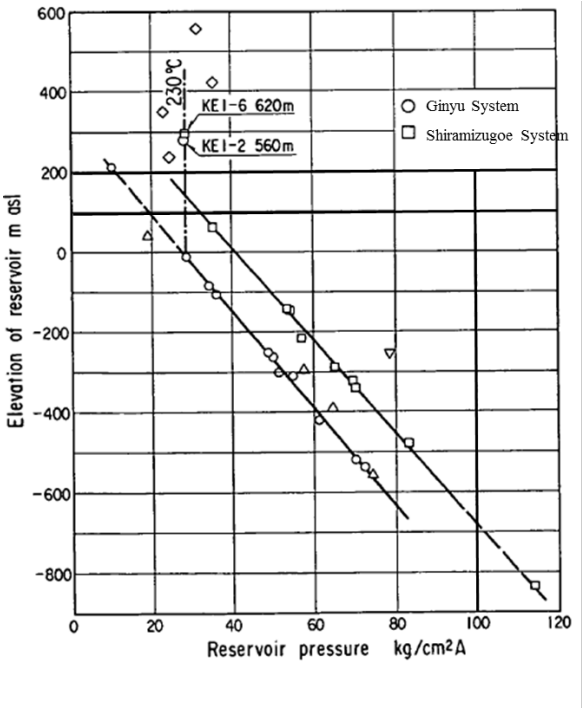

Figure 2: Reservoir pressure-elevation relationships for wells located in the Ogiri field (Kodama and Nakajima, 1988).

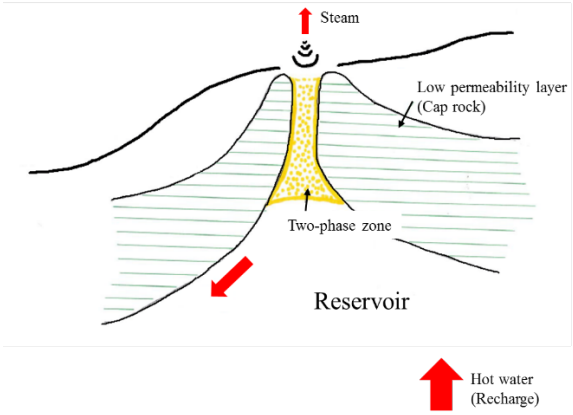

Figure 3: Conceptual model of the Ginyu reservoir (Yano and Ishido, 1995).

3. THREE DIMENSIONAL NUMERICAL MODEL

We began by improving the two-dimensional model developed by Yano et al. (1995). Our improved three-dimensional grid system covers an area of 2850 m x 700 m from elevations of 850 m a.s.l down to 1050 m b.s.l. The grid block size varies from 50 m x 100 m to 500 m x 200 m and the thickness of the vertical layers ranges from 30 m to 300 m. The east-west extension of the grid system is divided into 17 blocks and the north-south extent into 5 blocks. Depth is divided into 21 layers. The total number of grid blocks in the numerical model is 1785 and all grid blocks are treated as porous media.

We incorporated the important geological features such as cap rock into our numerical model. The upper parts of the model consists of the cap rock with lowest permeability value and in order to represent Ginyu fault the high permeable area was located passing through cap rock on the basis of geological data such as fumarole, steam-water two-phase zones and vapor-static relationship. We also set the deep recharge area and the horizontal conduit for discharge area at the west side of the model. The rocks surrounding the reservoir are more permeable than the cap rock, but their permeability is low enough so that conduction is the perceived dominant mode of heat transfer. Figure 4 shows the rock type in the vertical cross-section of the grid model describes as slice no., and Table 1 shows the physical properties for each rock type and the permeability is isotropic. The same density (2600 kg/m^3), wet heat conductivity (2.0 W/mK) and specific heat (1000 J/kgK) are assigned for all rock types. We used Grant's curves for the relative permeability values with water and steam residual saturation to be 0.3 and 0.05, respectively.

Table 1: Each rock physical properties in the numerical model

	Permeability (md)	Porosity(-)
Reservoir	500	0.5
High permeability area	40	0.1
Cap rock	0.02	0.01
Deep recharge area	100	0.1
Horizintal discharge area	40	0.1
Surrounded rock	1.0	0.1

Density (kg/m^3)	2600
Thermal Conductivity (W/m/K)	2.0
Specific Heat (J/kg/K)	1000

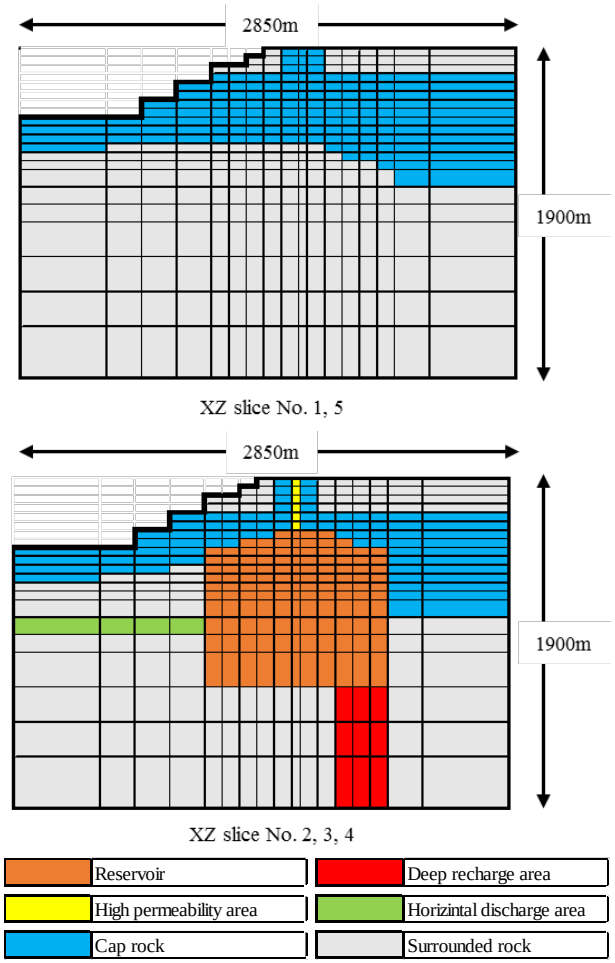

Figure 4: Assignment of rock types represented in the vertical cross-section. The y-dimension is divided into five slices; herein, labeled as slice no.

4. NATURAL STATE SIMULATION

4.1 Simulation conditions

We developed the numerical model using the TOUGH2 numerical simulator and used EOS4 as EOS (equation of state) modules. Firstly, we carried out a natural-state simulation to obtain the temperature and pressure distributions in the Ogiri geothermal area before exploitation. In the natural-state simulation, we compared simulated results with measured temperatures and pressure values at the feedpoint. These data were received from Nittetsu Mining Co., Ltd. The forward simulation was repeated until appropriate matches were obtained between measured and simulated values.

For initial conditions of natural-state simulation, a pressure equilibrium condition saturated with water at 10ºC was specified in each grid block. Boundary conditions are shown in Fig 5. For boundary conditions, constant pressure (= 0.1013 MPa) and temperature (10ºC) were assigned for all blocks, except at the top of the fracture which is kept at 100ºC as shown in Fig. 5 in yellow grid. The lateral boundaries of the model were impermeable to mass and adiabatic to heat except at the west side of the model where an outflow of fluid is allocated as shown in Fig. 5 in green grid. The outflow rate was calculated by using a productivity index (PI) and well-bottom pressure (P_{wb}). A mass recharge with temperature of 240ºC and the total flow rate of 9 kg/s was specified at nine locations in the bottom layer as indicated in red grids in Fig.5. Two values of conductive heat flux were also prescribed at the bottom of the model: 0.209 W/m^2 in the bottom layer in the eastern part and 0.0936 W/m^2 in western part.

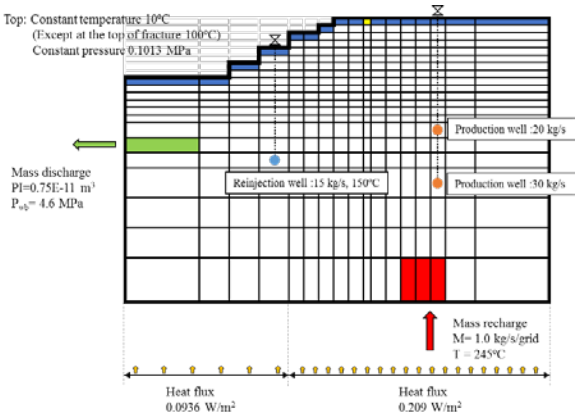

Figure 5: Boundary conditions for the three-dimensional model.

We examined the effects of the capillary pressure on the development of the two-phase zone in the shallower parts of the reservoir. Four models were used in this study with different capillary pressure values. Expression for capillary pressure varies for the reservoir and other rock structures. The reservoir capillary pressure is described by Eq. (1), an expression that was utilized by Pruess and O'Sullivan (1992) for the fracture blocks in his study, while the capillary pressure for the other rock structure is described by Eq. (2) where P_c is the capillary pressure, A is the maximum fracture pressure in kPa, S_l is the liquid saturation, S_{ef} is the effective liquid saturation, which is given by Eq. (3), and P_o and λ are the constant factors. Eq. (2) was used for two-phase model by Van Genuchten (1980). The capillary pressure functions used in the different models are shown in Table 2 as a function of liquid saturation and Fig. 6 shows plots of capillary pressure vs liquid saturation for Model IV. Models II to IV indicate an increasing reservoir capillary pressure and Model I don't consider capillary pressure.

$$P_c = -A(S_l) + A \quad (1)$$

$$P_c = P_o(S_{ef}^{-1/\lambda} - 1)^{1-\lambda} \quad (2)$$

$$S_{ef} = \frac{S_l - S_r}{1 - S_r} \quad (3)$$

Table 2: The capillary pressure used for the different models

Model	Reservoir P_c (kPa)	The other rocks P_c(kPa)
I	P_c=0	P_c=0
II	P_c=-500*S_l+500	P_c=100($S_{ef}^{-1/0.771}$-1)$^{0.229}$
III	P_c=-750*S_l+750	P_c=100($S_{ef}^{-1/0.771}$-1)$^{0.229}$
IV	P_c=-1000*S_l+1000	P_c=100($S_{ef}^{-1/0.771}$-1)$^{0.229}$

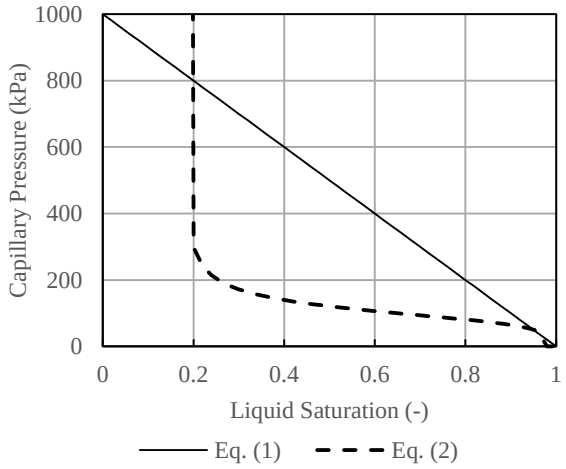

Figure 6: Comparison between Eq. (1) and Eq. (2) plots of capillary pressure vs liquid saturation for Model IV.

4.2 Results

Results of Model I-IV do not have significant variation in terms of temperature and pressure values in the natural-state simulation. In this regards, only the results of Model I are shown in Figs 7-10. Figure 7 presents the distribution of temperature in the X-Z slice No.3 in color gradient, and the movement of liquid fluid in the model as represented by arrow vectors. It was found that the fluid mainly flow in the reservoir and conduits because of the lower permeability of the cap rock and the surrounding rock. Figures 8 and 9 show the comparison between measured and computed natural-state temperature and pressure profiles respectively for the wells, located in the reservoir. The computed temperature is high at the shallower depth but exhibits a reasonable match at deeper levels as seen in Fig 8. Figure 9 shows that a vapor-static pressure profile is obtained in the upper parts of the model and that a good match between measured and computed values of pressure in the reservoir is observed. These figures indicate reasonable matches in natural-state simulation.

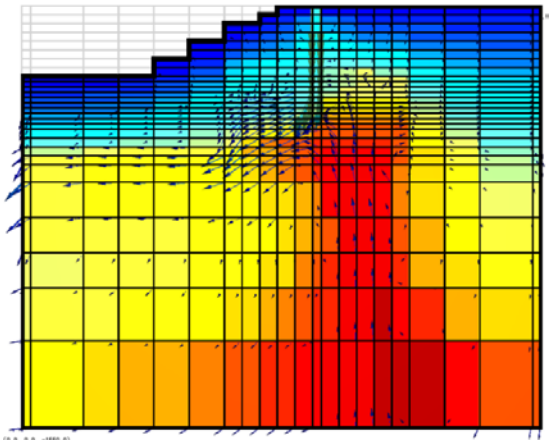

Figure 7: Distribution of temperature and liquid fluid flow in the X-Z slice No.3.

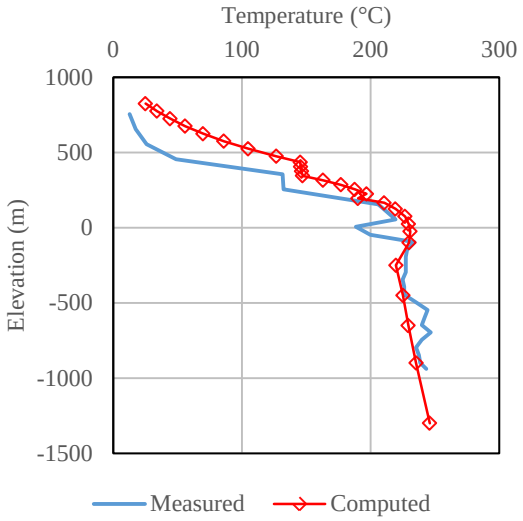

Figure 8: Comparison between measured and computed temperature profile.

Figure 10 shows the distribution of steam saturation in the X-Z slice No.3. Steam-water two-phase zones are observed to form in the shallow part of the reservoir. This deduces to two-phase zones to have developed in the shallow part of the model. Figure 10 also shows that the two-phase zones are not well developed outside the reservoir. Tsypkin and Calore (1999) found that steam/water capillary pressure could play a stabilizing role for the vaporization front, causing a drastic change in the steam saturation to develop. Urmeneta (1997) also found that capillary pressure tended to keep the steam phase in the fractures. Figure 11 shows the steam saturation distribution in the cross-section of the reservoir rock that corresponds to the depth from +475m a.s.l. down to +225m a.s.l. for Models I-IV. It was concluded that the steam saturation decreases with increasing capillary pressure, then spread of the steam-water two-phase zones have different distribution manner in each model as shown in Fig 11.

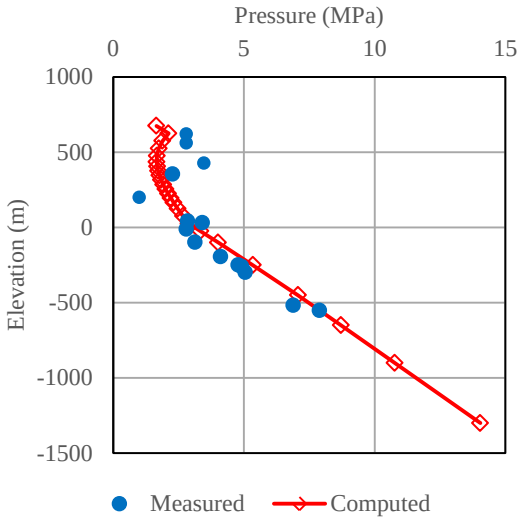

Figure 9: Comparison between measured and computed pressure profile.

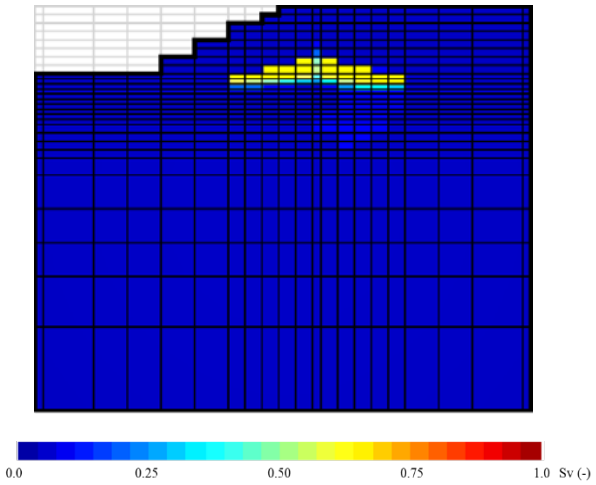

Figure 10: Distribution of steam saturation in the X-Z slice No.3.

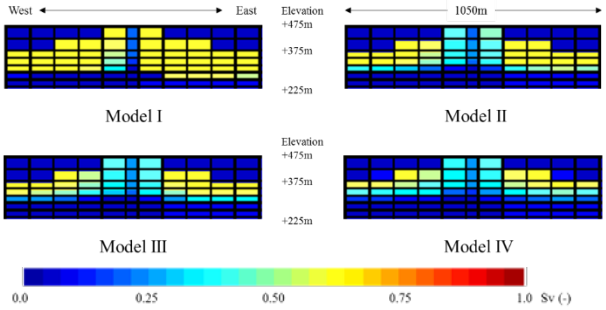

Figure 11: Distribution of steam saturation of each model in the shallow parts of the reservoir rocks

5. PRODUCTION AND REINJECTION SIMULATION

5.1 Simulation conditions

Results of the temperature and pressure distribution obtained from the natural-state simulation was used as initial conditions for the production and reinjection simulation. Boundary conditions were same the same with that of natural-state simulation. In this study, we conducted simplified simulation so that we set the production wells one by one into the deep and shallow points of the eastern reservoir and also set the reinjection well in the western part of the reservoir. The shallow and deep production rates were set to 6.0 kg/s and 12.0 kg/s respectively. The reinjection rate ranging from 25% to 100% of the total production rate (18.0 kg/s) were used and the temperature was set to 150ºC. We set the calibration time to 20 years. We studied how capillary pressure affects the reservoir behavior by comparing the results of analysis of temporal changes in temperature and pressure in the Model I-IV.

5.2 Results

Computed pressure and temperature values at -100m a.s.l. of the reservoir through time with variable reinjection rate are shown in Fig. 12 and 13 respectively. It can be seen in Fig. 12 that the reinjection is contributing into reservoir sustainability, because the pressure drop of the reservoir is reduced as amount of reinjection rates increases. Since the amount of the pressure drop is smaller in the order of Model I, II, III and IV, we find that the reservoir pressure is likely slower decrease as the capillary pressure is increased. The same trend can be observed for temperature changes with time in Fig. 13. Figure 13 also shows that the temperature gradient of each model increase after 10-15 years. It is considered that these tendencies are related to formation of steam-water two-phase zones, and computed steam saturation changes at the same block with time are shown in Fig. 14. However, Fig. 14 shows only the result of 25 % reinjection rate of each model. It can be seen that the time of the sharp drop in temperature and of the formation of the two-phase zones match in Fig. 13 and 14.

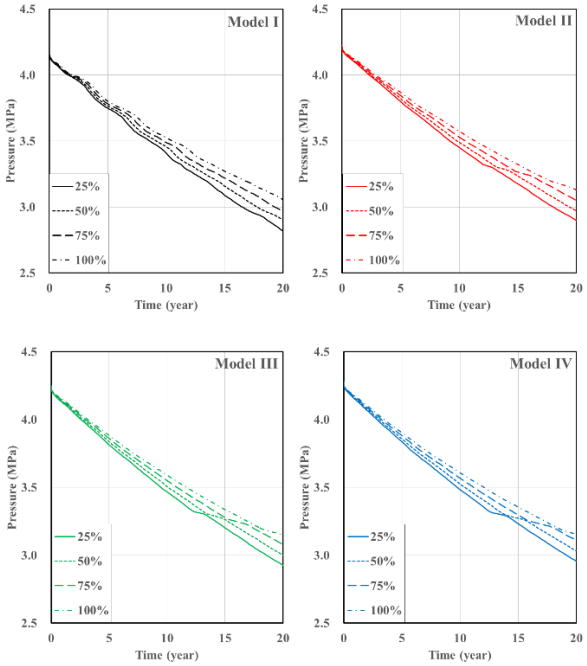

Figure 12: Time-dependent change of reservoir pressure at -100m a.s.l. for different reinjection rates.

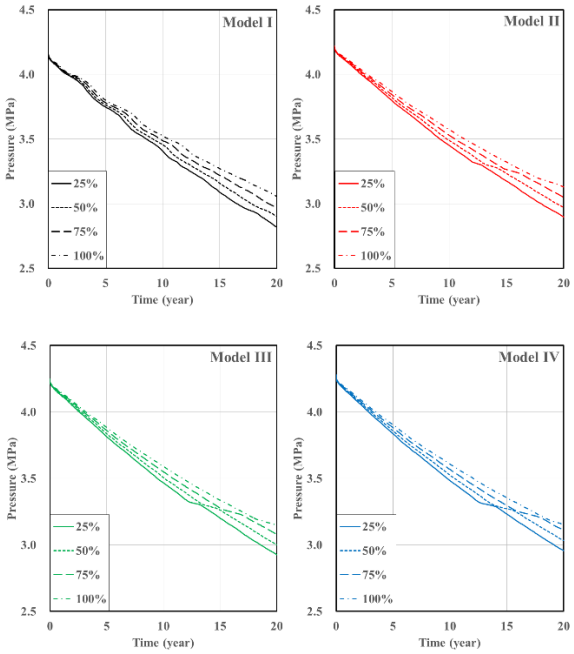

Figure 13: Time-dependent change of reservoir temperature at -100m a.s.l. for different reinjection rates.

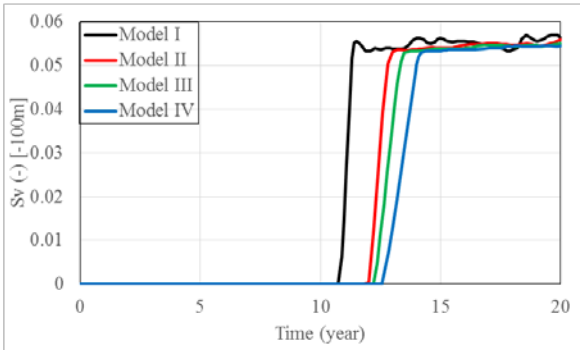

Figure 14: Time-dependent change of steam saturation at -100 m a.s.l. for each model.

Next, we studied the effects of the capillary pressure to the behavior of steam-water two-phase zones in the shallower parts of the reservoir. Figure 15 shows the value of steam saturation at 200 m a.s.l. of the reservoir with time. It can be seen that vapor pressure lowering occurs by considering the capillary pressure, and that the relationship between the capillary pressure and the vapor pressure lowering is described by the Kelvin's equation (4) where R is the universal gas constant, T is the absolute temperature, ρ is the liquid density, M is molecular weight of water, P_{sat} is the saturation vapor pressure and P_v is the lowered vapor pressure.

$$P_c = \frac{RT\rho}{M}\ln\left(\frac{P_{sat}}{P_v}\right) \qquad (4)$$

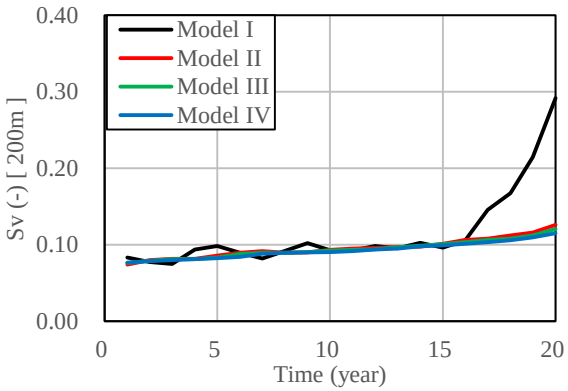

Figure 15: Time-dependent change of steam saturation at +200 m a.s.l. for each model.

Because of the vapor pressure drop equilibrium of the reservoir pressure is less than the saturation vapor pressure, liquid phase is more stable than steam phase. The water molecules absorbed in the pores of the rock by the capillary pressure are forced from the faces of the rock, so the potential of accumulation of water molecules in matrix area will be reduced. In the result, it can be seen that there is large difference of the steam saturation with time between Model I, which didn't consider capillary pressure, and the other models. It is also found that there are small differences between Models II-IV, which means that steam saturation gradually decreases as the capillary pressure increases. This is due to increasing water condensation in the pores with the increase in the relative pressure (Pv/Psat).

6. CONCLUSIONS

Numerical simulations of the Ginyu geothermal reservoir using a three-dimensional model was carried out to examine the effects of capillary pressure to the steam-water two-phase zones behavior. Results are summarized as follows:

1. In the natural-state simulation, the steam saturation of Model I, which did not include capillary pressure, was larger compared to the other models. Model I also had a narrow extension in the depth direction of the steam-water two-phase zones.

2. In the production and reinjection simulation, it was found that capillary pressure is a factor affecting reservoir pressure and temperature; such that the decrease rate of the reservoir pressure and temperature with time increased as the capillary pressure increased.

3. By introducing capillary pressure into the model, Model II-IV maintained smaller values of steam saturation with time than Model I due to less water molecules absorption in pores.

ACKNOWLEDGEMENTS

The authors would like to thank Nittetsu Mining Co., Ltd. for their support and for permission to use their data.

REFERENCES

Kodama, M. and Nakajima, T. (1988) *"Exploration and Exploitation of the Kirishima Geothermal Field."* Jpn. Geotherm. ASS. 25, **201** [in Japanese].

M.T. Van Genuchten. "A Closed-Form Equation for Predicting the Hydraulic Conductivity of Unsaturated Soils." Soil Sci. Soc. Am. J., Vol. 44, 1980, pp. **892-898**

Pruess, K. and O'Sullivan, M. *"Effects of Capillary and Vapor Adsorption in the Depletion of Vapor-Dominated Geothermal Reservoirs"*, Proc. of the 17th Annual Workshop on Geothermal Reservoir Engineering, Stanford University, California, January, 1992, **165**

Tsypkin, G. G. and Calore, C. *"Capillary Pressure Influence on Water Vaporization in Geothermal Reservoirs"*, Proc., Workshop on Geothermal Reservoir Engineering, Stanford University, California, January, 1999, **359**.

Urmeneta, N. A., Fitzgerald, S., and Horne, R. N. *"The Role of Capillary Forces in Natural State of Fractured Geothermal Reservoirs"*, Proc., Workshop on Geothermal Reservoir Engineering, Stanford University, California, January, 1998, **100**.

Yano, Y. and Ishido, T. *"Numerical Modeling of the Evolution of Two-Phase Zones under a Fractured Caprock"*, Geothermics Vol. 24, No. 4, 1995, **507**